

Thermal Conductivity of Suspensions Containing Nanosized SiC Particles

H. Xie,^{1, 2} J. Wang,¹ T. Xi,¹ and Y. Liu¹

Received February 7, 2001

Nanosized SiC suspensions were prepared, and their thermal conductivities were measured using a transient hot-wire method. The experimental results showed that the thermal conductivities of the studied suspensions were increased as expected, and the enhancement was proportional to the volume fraction of the solid phase, but the increasing ratio of the thermal conductivity was not significantly related to the base fluid. The effects of the morphologies (size and shape) of the added solid phase on the enhancement of the thermal conductivity of the nanoparticle suspension are reported for the first time.

KEY WORDS: hot-wire method; SiC nanoparticle suspension; thermal conductivity.

1. INTRODUCTION

The low thermal conductivity of a conventional fluid is a fundamental limit in the high compactness and effectiveness of heat exchangers, although considerable previous research and development have been focused on industrial heat transfer requirements. It is a strong need to develop advanced fluidic working media with substantially higher thermal conductivities, that is, improved heat transfer efficiency, and excellent fluidic characteristics. An innovative way of improving the thermal conductivity of a fluid is to suspend ultrafine metallic or nonmetallic solid powder in the fluid since the thermal conductivities of most solid materials are higher than those of liquids. Theoretical and experimental studies of the thermal conductivity of a suspension containing solid particles have been reported previously [1–3]. The suspensions in these studies have significantly higher thermal

¹ Shanghai Institute of Ceramics, Chinese Academy of Sciences, Shanghai 200050, China.

² To whom correspondence should be addressed. E-mail: huaqing_xie@hotmail.com

conductivities than the base fluids without solid particles. Unfortunately, suspended particles of micrometer or even millimeter dimensions may cause some severe problems, such as abrasion and clogging in small passages. Furthermore, the stabilities of all large-particle suspensions are very poor since the coarse-grained solid particles involved in suspensions settle out eventually.

The extensive research conducted on nanosized powders and the associated preparation and processing technology have provided insight into this problem in recent years. Nanoparticle suspensions are expected to exhibit excellent properties which conventional fluidic media and suspensions containing coarse-grained solid particles do not have. Because of the large surface area and enhanced heat capacity of nanocrystalline materials [4–6], nanoparticle suspensions will undoubtedly improve the heat transfer capacities. Also, the Brownian movement of nanoparticles in nanofluids helps to make the suspension stable [7]. Furthermore, nanoparticles can act as a lubricating medium because of their small sizes [8].

Thermal conductivities of nanoparticle suspensions have been reported by Masuda et al. [9], Lee et al. [10], and Wang et al. [11]. With the addition of a small amount of metal or metal oxide nanosized particles in fluids, the thermal conductivities of suspensions have been increased over those of base fluids. Choi [12], Xuan et al. [13], and Wang et al. [11] investigated the enhanced heat transfer mechanism of nanosized particle suspensions. Lee [14] used a nanosized metal particle suspension as a new coolant in a microchannel heat exchanger for the first time. He concluded that the nanoparticle suspension offered significant benefits. Pak and Cho [15] studied heat transfer enhancement in a circular tube using a nanoparticle suspension as the flowing medium. In their studies, γ - Al_2O_3 and TiO_2 were dispersed in water, and the Nusselt number was found to increase with an increase in the volume fraction and Reynolds number.

In the present work, spherical SiC particles with an average diameter of 26 nm and cylindrical SiC particles with an average diameter of 600 nm were dispersed in distilled water ($\text{DI-H}_2\text{O}$) and ethylene glycol (EG) separately at volume fractions up to 4.2%. Thermal conductivities of suspensions were measured by the transient hot-wire technique. Experimental results are compared with calculated values by a theoretical model, and the validity of this model is evaluated. The possible mechanism of the thermal conductivity enhancement in nanoparticle suspensions is discussed.

2. EXPERIMENTAL

2.1. Sample Preparation and Characterization

SiC particles with an average diameter of 26 nm (SiC-26) used in the present experiments were prepared by the laser-induced vapor-deposition

Table I. Morphologies of SiC Powders

	SiC-26	SiC-600
Average size	26 nm	600 nm
Particle shape	Spherical	Cylindrical

method using SiH_4 and C_2H_4 as sponsors. SiC nanoparticles were prepared with excess carbon to reduce oxidation at the particle surface. Since the existing free carbon powder can reduce the stability of suspensions and consequently affect their application [16], SiC nanoparticles used for producing suspensions were heated at 650°C for 30 min, leached with a 5% HF solution, and then repeatedly washed with deionized water to eliminate the excess carbon and the silica layer. The SiC powder used, with an average diameter of 600 nm (SiC-600), was bought commercially and had a low impurity. Transmission electron microscopy (TEM) was used to characterize the SiC powders. The morphologies of the SiC powders are listed in Table I.

Nanoparticle suspensions were prepared by a two-step method, in which SiC particles were produced first, followed by a second step in which the powders were dispersed into a base fluid in a mixing container. SiC particles were deagglomerated by intensive ultrasonication after being mixed with base fluid, and then the suspensions were homogenized by magnetic force agitation.

To investigate the effects of the volume fraction, the size and shape of the solid phase, and the conductivity of the base liquids systematically, four series of solid particle suspensions were produced. These four series consisted of SiC-26 in water, SiC-26 in EG, SiC-600 in water, and SiC-600 in EG separately, with a solid particle volume fraction of a maximum of 4.2%.

2.2. Measurement of the Thermal Conductivity of Nanoparticle Suspensions

The samples measured in our experiments are electrically conductive, so a transient hot-wire cell and an electrical system were designed. According to the principle presented by Nagasaka and Nagashima [17], the thermal conductivities of measured fluids, λ , can be determined by the following formula:

$$\lambda = \left(\frac{q}{4\pi} \right) \left/ \left(\frac{d(\Delta T_w(\tau))}{d(\ln \tau)} \right) \right. \quad (1)$$

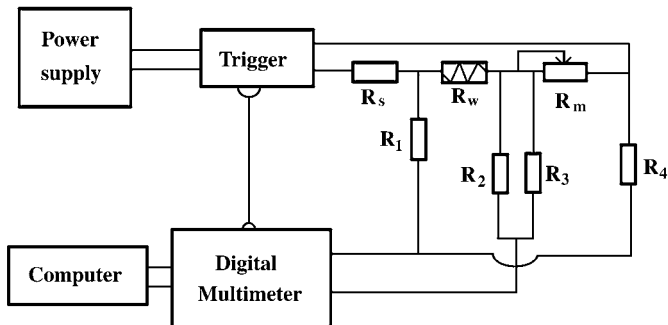


Fig. 1. Block diagram of the electrical system.

where q is the applied heating power per unit, τ is the heating time, and $\Delta T_w(\tau)$ is the temperature rise of the hot wire.

The hot-wire cell used here is similar to the cell reported by Lee et al. [10]. A platinum wire with a diameter of $20\ \mu\text{m}$ was used for the hot wire, and it served as both a heating unit and a resistance thermometer. The wire was coated with a $5\text{-}\mu\text{m}$ -thick electrical insulation layer, and it was welded to rigid copper supports. The welded spots were coated with an epoxy adhesive with excellent electrical insulation and heat conduction. The ratio of wire length to diameter was very high (the length was about $130\ \text{mm}$) to eliminate the effect due to axial conduction at both ends of the wire.

A block diagram of the designed electrical system is shown in Fig. 1. In this diagram, R_w is the resistance of the metallic wire, R_m is a $15\ \Omega$ potentiometer, R_s is a standard resistor of $200\ \Omega$ used to stabilize the DC current supply for R_w , and R_1 , R_2 , R_3 , and R_4 are high-resolution standard resistors of $30\ \text{k}\Omega$. The resistance of R_m is adjusted to allow the offset voltage from the Kelvin bridge at initial equilibrium to be canceled, and then the voltage offset caused by a change in R_w can be recorded with a Keithley 2000 digital voltmeter at a sampling rate of five per second. The recorded data are transferred to a PC and then processed. The uncertainty is estimated to be $\pm 0.5\%$ in these measurements.

3. RESULTS AND DISCUSSION

3.1. Thermal Conductivity of SiC Particle Suspensions

To minimize temperature fluctuations, the hot-wire cell containing the measured sample was placed in a thermostatic air bath at a controlled temperature of 4°C , when the thermal conductivity measurements were performed.

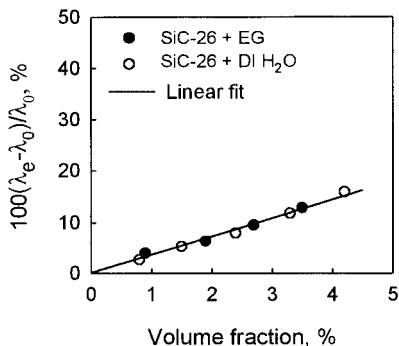


Fig. 2. Enhancement of the thermal conductivities of SiC-26 suspensions.

The thermal conductivity enhancement of SiC-26 suspensions as a function of the solid-phase volume fraction is shown in Fig. 2, where λ is the thermal conductivity, and the subscripts e, p, and 0 represent the effective, particle, and base fluid, respectively. The results show that the thermal conductivities of the suspensions containing a small amount of nanoparticles are substantially higher than those of the base fluids without nanoparticles. For SiC-26 in DI-H₂O suspension, the thermal conductivity can be increased by about 15.8% at a volume fraction of 4.2%.

The thermal conductivity increase ratios of SiC-600 suspensions as a function of the solid-phase volume fraction is shown in Fig. 3. It can be seen that a significant enhancement of the thermal conductivity takes place if a small amount of SiC particles is added to the base fluid. For SiC-600 in

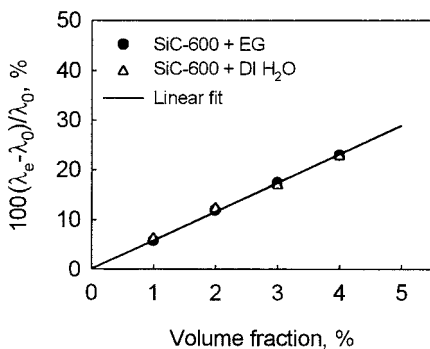


Fig. 3. Enhanced thermal conductivities of suspensions containing SiC-600.

DI-H₂O, the thermal conductivity can be increased by 22.9% at a volume fraction of 4%.

The measured data clearly indicate that the ratios of the thermal conductivities of the suspensions increase almost-linearly with the volume fraction. Lee et al. [10] showed experimentally that the thermal conductivities of nanoparticle suspensions depended on the thermal conductivity of base fluids. They argued that the conductivity ratio increases for Al₂O₃ or CuO in an EG suspension system were always higher than those of the same nanoparticles in a water suspension system [10]. However, our experimental results in Figs. 2 and 3 for the increase in the thermal conductivity ratio show no significant difference between suspension systems with the same solid particles in different base fluids. That is, the thermal conductivity increase for SiC in EG is very close to that for the same type of particles in DI-H₂O at the same solid volume fraction.

To emphasize the effect of particle morphology, the thermal conductivity ratios of two suspension systems, consisting of SiC-26 and SiC-600 in DI-H₂O, are shown in Fig. 4. The enhancement ratios of SiC-26 in DI-H₂O are obviously lower than those of SiC-600. The only difference between the two suspension systems is on the particle morphology (shape and size). Here the particle shape affects heat transfer between the solid particles and the base liquid. The mechanism is investigated in the next section.

3.2. Comparison with the Empirical Model

Because of the absence of a theory for calculating the thermal conductivity of nanoparticle suspensions, existing equations for a solid/liquid system were applied to compare the predicted values with the experimental

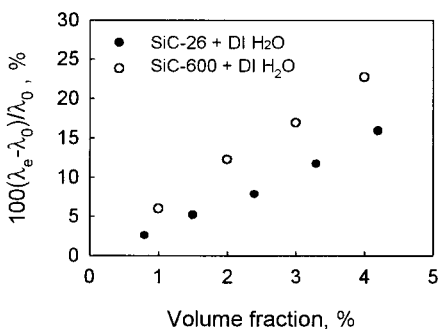


Fig. 4. Thermal conductivity ratios of suspensions containing different solid particles.

data. Maxwell's equation [18] was the first approach for computing the effective electrical conductivity of a random suspension of spherical particles. Because of the identical dimensionless formulations, the thermal conductivity could be calculated in the same way as the electrical conductivity, dielectric constant, and magnetic permeability of mixtures. A second-order formulation extended from Maxwell's result was developed by Jeffrey [19] and later modified by several authors [20, 21]. Numerical simulation conducted by Bonnecaze and Brady [22, 23] showed that, for random dispersion of spheres, the simulated results agreed well with Jeffrey and Maxwell's equations at low solid volume fractions. Hamilton and Crosser [2] developed a complicated model to predict the thermal conductivity of suspensions containing micrometer- or millimeter-size particles. All of the equations mentioned above have been successfully verified by experimental data for mixtures with large-size particles and at low concentrations. The difference between the measured data and the prediction is less than a few percent when the volume fraction of the dispersed phase is less than 20%.

The Hamilton and Crosser equation for computing the thermal conductivity of suspensions was applied since this model considers the effect of the shape as well as that of the volume fraction of the dispersed particle. The equation is expressed as

$$\lambda_e = \lambda_0 \left[\frac{\lambda_p + (n-1) \lambda_0 - \alpha(n-1)(\lambda_0 - \lambda_p)}{\lambda_p + (n-1) \lambda_0 + \alpha(\lambda_0 - \lambda_p)} \right] \quad (2)$$

where α is the volume fraction of the particle and n is the shape factor. It can be calculated empirically by

$$n = 3/\psi \quad (3)$$

where ψ is the sphericity, which is defined by the ratio of the surface area of a particle to that of a sphere with the same volume as the particle. For example, the sphericity of a spherical particle is 1, while that of a cylindrical particle is 0.5. So the smaller the sphericity of the particle, the larger the shape factor will be.

Sphericities of 1 and 0.5 were used for SiC-26 and SiC-600, respectively, in the Hamilton and Crosser equation to calculate the effective thermal conductivities. The computed results for SiC-26 and SiC-600 suspensions, together with experimental data, are shown in Figs. 5 and 6. From these figures, it can be seen that the experimental results for SiC-600 suspensions are consistent with the predicted values, while those for SiC-26 suspensions are obviously greater than the calculated values.

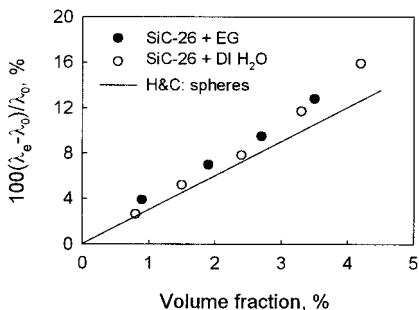


Fig. 5. Measured and calculated thermal conductivities of SiC-26 suspensions.

In the calculation, the thermal conductivities of the base fluids were taken as $0.261 \text{ W} \cdot \text{m}^{-1} \cdot \text{K}^{-1}$ for EG and $0.573 \text{ W} \cdot \text{m}^{-1} \cdot \text{K}^{-1}$ for DI- H_2O . We used a bulk value of $490 \text{ W} \cdot \text{m}^{-1} \cdot \text{K}^{-1}$ for SiC particles because no data were available for nanoparticles. It is well known that, in the micro- and nano-scale regimes, the thermal conductivity is much lower than the bulk value, because of boundary scattering of phonons and/or electrons [24, 25]. It is expected that the thermal conductivity of a nanoparticle suspension is reduced. However, as shown in Fig. 5, the measured thermal conductivity is about 20% greater than the value calculated using an existing model even when the thermal conductivity of SiC-26 is taken as a bulk value. Therefore, the theoretical models, which successfully predict the thermal conductivities of large-size particle suspensions, cannot be used to calculate the effective thermal conductivity of a nanoparticle suspension.

Because heat transfer between the particles and the fluid takes place at the particle–surface interface, it is expected that heat transfer will be more efficient and a rapid for a system with a larger interfacial area. If the size of

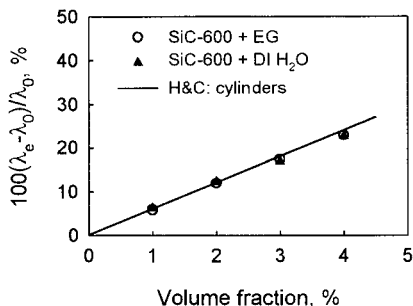


Fig. 6. Measured and calculated thermal conductivities of SiC-600 suspensions.

the dispersed particles is large, what matters is the volume of the particles. The Hamilton and Crosser model focuses on the effect of the particle shape on the surface area. Therefore, for the SiC-600 suspensions, the Hamilton and Crosser model is capable of predicting the thermal conductivities. SiC-26 particles have a larger surface area per volume, therefore, their suspensions have a larger particle-liquid interfacial area. An improvement in the effective thermal conductivities of suspensions is expected when the dispersed particle size decreases.

4. CONCLUSIONS

To investigate the thermal conductivity behavior of SiC dilute nanoparticle-fluid mixtures, the thermal conductivities of four series suspensions were measured by a transient hot-wire method.

The present experiments show that the thermal conductivities of the SiC suspensions, containing a small amount of solid particles, are significantly higher than those of the base liquids. In the low volume fraction range, the thermal conductivity enhancing ratios increase almost-linearly with the volume fraction of solid particles. For different systems containing the same kind of particles, the thermal conductivity ratios are independent of the base liquids, but the absolute value of the thermal conductivity of the suspension is proportional to that of the base liquids. For systems with the same base liquid, the morphology of solid particles affects predominantly the enhancement ratios.

The measured results have been compared with the predicted values of a model developed by Hamilton and Crosser [2]. The model is capable of predicting the thermal conductivity of a large-size SiC-600 particle suspension. However, it appears to be inadequate for suspensions containing nanosized SiC-26 particles. To explain this discrepancy, further investigation on the effect of particle size is needed.

ACKNOWLEDGMENT

The authors thank the Natural Science Foundation of China (Project No. 50006014) for financial support.

REFERENCES

1. A. S. Ahuja, *J. Appl. Phys.* **46**:3408 (1975).
2. R. L. Hamilton and O. K. Crosser, *I & EC Fund.* **1**:187 (1962).
3. K. V. Liu, U. S. Choi, and K. E. Kasza, *Argonne National Laboratory Report ANL-88-15* (1988).

4. J. Rupp and R. Birringer, *Phys. Rev. B* **36**:7888 (1987).
5. H. Gleiter, *Prog. Mater. Sci.* **33**:223 (1989).
6. H. Zhang and J. F. Banfield, *J. Mater. Chem.* **8**:2073 (1998).
7. L. Zhang and J. Mou, *Nanoscale Material Sciences* (Liaoning Sci. Technol. Press, Liaoning, 1994) [in Chinese], p. 44.
8. Z. S. Hu and J. X. Dong, *Wear* **216**:92 (1998).
9. H. Masuda, A. Ebata, K. Teramae, and N. Hishinuma, *Netsu Bussei* (Japan) **7**:227 (1993).
10. S. Lee, U. S. Choi, S. Li, and J. A. Eastman, *J. Heat Transfer* **121**:280 (1999).
11. X. Wang, X. Xu, and U. S. Choi, *J. Thermophys. Heat Transfer* **13**:474 (1999).
12. U. S. Choi, *Developments and Applications of Non-Newtonian Flows*, D. A. Singiner and H. P. Wang, eds. (ASME, New York, 1995), FED-Vol. 231.
13. Y. Xuan and Q. Li, *Int. J. Heat Fluid Flow* **21**:58 (2000).
14. S. Lee and U. S. Choi, *Recent Advance in Solids/Structures and Application of Metallic Materials*, Y. Kwon, D. Davis, and H. Chung, eds. (ASME, New York, 1996), MD-Vol. 72, p. 227.
15. B. C. Pak and Y. I. Cho, *Exp. Heat Transfer* **11**:151 (1998).
16. P. Tartaj, M. Reece, and J. S. Moya., *J. Am. Ceram. Sci.* **81**:389 (1999).
17. Y. Nagasaka and A. Nagashima, *J. Phys. E Sci. Instrum.* **14**:1435 (1981).
18. J. C. Maxwell, *Electricity and Magnetism, Part II*, 3rd ed. (Clarendon, Oxford, 1904), p. 440.
19. D. J. Jeffrey, *Proc. Roy. Soc. (London) Ser. A* **335**:355 (1973).
20. S. Lu and H. Lin, *J. Appl. Phys.* **79**:6761 (1996).
21. R. H. Davis, *Int. J. Thermophys.* **7**:609 (1986).
22. R. T. Bonnecaze and J. F. Brady, *Proc. Roy. Soc. (London) Ser. A* **430**:285 (1990).
23. R. T. Bonnecaze and J. F. Brady, *Proc. Roy. Soc. (London) Ser. A* **432**:445 (1991).
24. K. E. Goodson, M. I. Filk, L. T. Su, and D. A. Antoniadis, *J. Heat Transfer* **116**:317 (1994).
25. D. G. Cahill, H. E. Fischer, T. Klister, E. T. Swartz, and R. O. Phol, *J. Vac. Sci. Tech. A* **7**:1259 (1989).